Molecular Crystals and Liquid Crystals
Publication details, including instructions for authors and subscription information:
http://www.tandfonline.com/loi/gmcl20

Anomalous Diffusion Effects on the Electrical Impedance Response of Liquid-Crystalline Systems

P. A. Santoro [a], E. K. Lenzi [a], L. R. Evangelista [a], F. Ciuchi [b], A. Mazzulla [b] & N. Scaramuzza [c]

[a] Departamento de Física, Universidade Estadual de Maringá, Avenida Colombo, 5790, 87020-900, Maringá, Paraná, Brazil

[b] CNR-IPCF UoS di Cosenza, Licryl Laboratory, and Centro di Eccellenza CEMIF.CAL, Università della Calabria, 87036, Arcavacata di Rende, Italy

[c] Dipartimento di Fisica, Università della Calabria, 87036, Arcavacata di Rende, Italy

Published online: 14 Jun 2013.

To cite this article: P. A. Santoro, E. K. Lenzi, L. R. Evangelista, F. Ciuchi, A. Mazzulla & N. Scaramuzza (2013) Anomalous Diffusion Effects on the Electrical Impedance Response of Liquid-Crystalline Systems, Molecular Crystals and Liquid Crystals, 576:1, 23-31, DOI: 10.1080/15421406.2013.789423

To link to this article: http://dx.doi.org/10.1080/15421406.2013.789423

Mol. Cryst. Liq. Cryst., Vol. 576: pp. 23–31, 2013

ISSN: 1542-1406 print/1563-5287 online
DOI: 10.1080/15421406.2013.789423

Taylor & Francis
Taylor & Francis Group

Anomalous Diffusion Effects on the Electrical Impedance Response of Liquid-Crystalline Systems

P. A. SANTORO,[1,*] E. K. LENZI,[1] L. R. EVANGELISTA,[1]
F. CIUCHI,[2] A. MAZZULLA,[2] AND N. SCARAMUZZA[3]

[1]Departamento de Física, Universidade Estadual de Maringá, Avenida Colombo, 5790, 87020-900, Maringá, Paraná, Brazil
[2]CNR-IPCF UoS di Cosenza, Licryl Laboratory, and Centro di Eccellenza CEMIF.CAL, Università della Calabria, 87036, Arcavacata di Rende, Italy
[3]Dipartimento di Fisica, Università della Calabria, 87036, Arcavacata di Rende, Italy

The electrical impedance response of six nematic liquid crystals samples is analyzed by means of an extension of the Poisson-Nernst-Planck diffusional model. This formulation includes fractional derivatives of distributed order governing the behavior of the bulk density of mobile charges, whose solutions are subjected to integro-differential equations accounting for the boundary conditions. The role of the intrinsic surface lengths involved in the adsorption-desorption phenomena at the electrodes is emphasized, in order to analyze the frequency dependence of the real and imaginary parts of the electrical impedance experimentally obtained.

Keywords Impedance; ionic conduction; admittance

PACS: 84.37.+q; 77.22.−d; 66.10.Ed

1. Introduction

Liquid crystals (LC) are insulating materials whose finite resistance comes from the ionic impurities dissolved in the medium [1]. These mobile ionic charges are responsible for important contributions to their dielectric properties. In displays, the ions can change the resistance of the material and may be connected with different phenomena such as low VHR (voltage holding ratio) and image sticking [2,3]. When an LC sample is submitted to an alternating current (AC), the presence of ions will play a decisive role in the electrical impedance response of the material, specially at low frequencies, where the time scales involved allow for strong surface effects, such as the adsorption-desorption phenomenon [1]. The electrical impedance or immittance spectroscopy is a powerful technique employed to analyse these materials and can provide information about the conductivity and the permittivity, which are particularly important for display applications [2].

In this paper, we analyse the impedance spectroscopy data of a series of LC systems by using an analytical expression for the electrical impedance obtained in the framework of a general physical model [4]. In this model, the mathematical problem of a diffusion

*Corresponding author: P. A. Santoro. Tel.: +55 44 3011 5979; Fax: +55 44 3263 4623. E-mail: psantoro@dfi.uem.br

Table 1. Sample thickness and polyimide layer in the inner surface of the cells.

Sample	AU2	AU10	AU20	ITO2	ITO10	ITO20
d (μm)	35.0	36.0	36.0	32.5	37.0	38.0
Polyimide (nm)	4	20	50	4	20	50

equation of distributed order [5] for the mobile ions coupled to the Poisson's equation for the electrical potential in the bulk is solved. The problem is characterized by boundary conditions expressed by means of an integro-differential equation. These boundary conditions embody, in particular, the usual kinetic equation for describing the adsorption-desorption process at the electrodes but is expressed in terms of a temporal kernel that, if appropriately chosen, can cover different scenarios, including also the effect of fractional derivatives on the boundary conditions. Indeed, the presence of these fractional derivatives in the time domain may lead to some kind of anomalous surface effects on the electrical response of the sample. For instance, one can consider the adsorption phenomena as governed by a fractional kinetic equation, which is well-tailored to account, in some way, for memory effects in the process. Likewise the choice of the kernel can account for chemisorption or physisorption process or both [6,7]. Furthermore, it can be also constructed to represent conditions of blocking or transparent electrodes, among other physically plausible conditions.

It is just this general character of the boundary conditions that permits one to face the high complexity of the experimental data regarding a series of different samples of LC in the nematic phase [8]. These samples have been prepared in such a way that the surface treatment change the aligning layers at the electrodes from one cell to the other in a prescribed and controlled way, thus permitting some kind of "systematic" investigation of these changes on the electrical response of the samples. The aim of this paper is therefore to present some concluding results of this systematic analysis by emphasizing the role of intrinsic lengths appearing in the approach in connection with the boundary conditions at the limiting electrodes.

2. Sample Preparation and Measurements

Six different samples have been prepared using liquid crystal 5CB (Merck) to fill cells provided with Mylar spacers. Rubbed polyimide was used as the alignment layer for the liquid crystal, where the layer thickness used was achieved by spin coating the substrates with 10 wt% solution of LQ1800 (Hitachi) in methyl pyrrolidinone. The electrode used consists of an evaporated gold or ITO pixel with surface area of 1×1 cm^2 (the samples are referred hereafter as AU2, AU10, AU20, ITO2, ITO10, and ITO20). Table 1 shows the polyimide layer thickness used in the surface treatment of the samples.

As described in preceding works [8,9], the complex impedance has been measured by a Potentiostat/Galvanostat/Impedentiometer EG & G Mod. 273A in a frequency range from 10^{-3} to 10^5 Hz. Low amplitude of the sinusoidal applied voltage was chosen, 25 mV rms, to avoid electrically induced reorientation of the liquid crystal. One connector acts as working electrode, while the counter electrode has been short-circuited with the reference one. Measurements at lower voltages give the same results but introduce more noise. Moreover, we are further below any 5CB threshold (dielectric reorientation or flexoelectric effect)

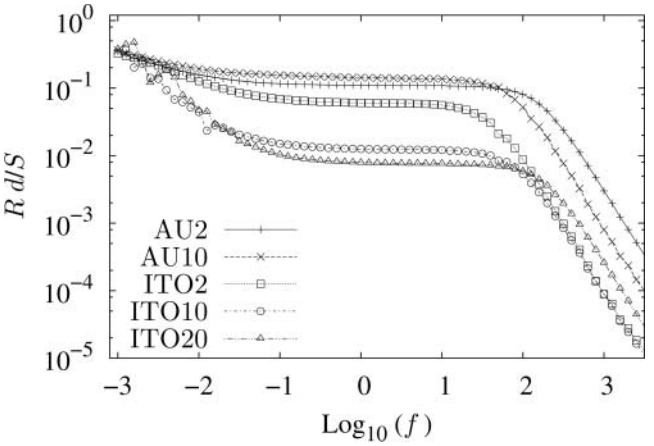

Figure 1. Real ($R = \mathrm{Re}\{Z\}$) part of the impedance Z, normalized by the maximum value in each of the experimental data sets. Here, d is the thickness of the cell and S is the surface area of the electrodes.

[2,3]. This assures that the linear approximation to be employed in the calculation of the electrical impedance works well and can be applied without further concerns.

In order to have a glimpse of the general characteristics of the samples analysed in this work, Figs. 1 and 2 show the real (R) and imaginary (X) parts of electrical impedance obtained experimentally as a function of the frequency.

By inspecting these figures, one can note that the behaviors of AU2, AU10, and ITO2 follow a similar trend. One can also see that the impedance curves for ITO10 and ITO20 are a little apart from the three previous mentioned samples. The impedance of AU20 sample has a peculiar, more complicated, behavior and for this reason it was analysed in a separated work (see details in Ref. [8]) and will not be considered in the present analysis.

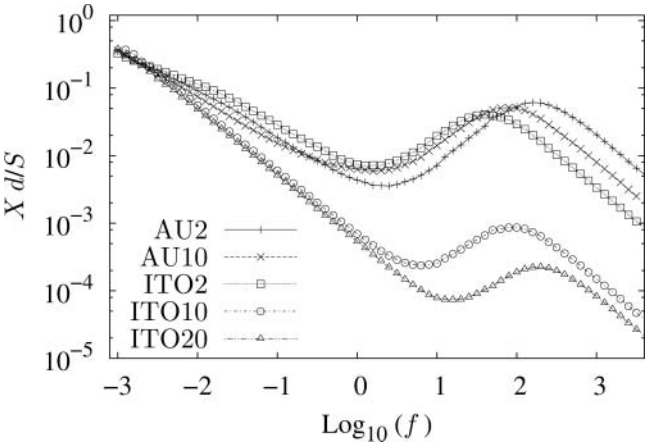

Figure 2. Imaginary ($X = -\mathrm{Im}\{Z\}$) part of the impedance Z, normalized by the maximum value in each of the experimental data sets. Here, d is the thickness of the cell and S is the surface area of the electrodes.

3. Theoretical Model: Fundamental Equations

The theoretical model is an extension of the Poisson-Nernst-Planck model including fractional derivatives of distributed order to account for the bulk behavior of the density of particles [10,11] and an integro-differential equation to account for the boundary conditions [4,8]. For completeness, we recall below the fundamental equations to be solved in the framework of this model [4]. The first of these equations is the fractional diffusion equation governing the bulk density of ions n_α ($\alpha = p$ for positive and $\alpha = n$ for negative ones),

$$\int_0^\infty d\gamma\, \tau(\gamma) \frac{\partial^\gamma}{\partial t^\gamma} n_\alpha(z,t) = -\frac{\partial}{\partial z} j_\alpha(z,t), \tag{1}$$

in which $\tau(\gamma)$ represents a weight function for γ while the current density for both types of ions is given by

$$j_\alpha(z,t) = -D\frac{\partial}{\partial z} n_\alpha(z,t) \mp \frac{qD}{k_B T} n_\alpha(z,t) \frac{\partial V}{\partial z}, \tag{2}$$

where D is the diffusion coefficient for the mobile ions (assumed here as the same for positive and negative ones) of charge q, $V(z,t)$ is the actual electric potential across the sample, k_B is the Boltzmann constant, and T is the absolute temperature. The typical sample has a shape of a slab, of thickness d, with the electrodes placed at the positions $z = \pm d/2$, of a Cartesian reference frame in which z is the axis normal to them. The fractional operator considered in Eq. (1) is the Caputo's one, defined as

$$\frac{\partial^\gamma}{\partial t^\gamma} n_\alpha(z,t) = \frac{1}{\Gamma(k-\gamma)} \int_{t_0}^t dt' \frac{n_\alpha^{(k)}(z,t)}{(t-t')^{1-\gamma+n}}, \tag{3}$$

with $k-1 < \gamma < k$ and $n_\alpha^{(k)}(z,t) \equiv \partial_t^k n_\alpha(z,t)$ [5]. To consider different diffusive regimes (i.e., different values of γ) for the same ion in the sample, a choice of the distribution $\tau(\gamma)$ for the fractional time derivative of distributed order has to be made in an appropriate manner. The possibility of having different regimes is expected to play an important role in reproducing the experimental data regarding the real and imaginary parts of the electrical impedance. Likewise, to be prepared to detect anomalous behavior in the experimental data, it is also appropriate to consider general boundary conditions to be satisfied by the solutions of Eq. (1). A general, physically plausible, expression that permits to cover significant experimental situations can be written as:

$$j_\alpha(z,t)|_{z=\pm\frac{d}{2}} = \pm \int_{-\infty}^t d\bar{t}\kappa(t-\bar{t}) \frac{\partial^\eta}{\partial \bar{t}^\eta} n_\alpha(z,\bar{t}) \Big|_{z=\pm\frac{d}{2}}. \tag{4}$$

The fractional operator in Eq. (4) may represent a fractional time derivative (if $\eta > 0$) or a fractional integral (if $\eta < 0$). The remaining fundamental equation of the model is the Poisson's equation

$$\frac{\partial^2}{\partial z^2} V(z,t) = -\frac{q}{\varepsilon} \left[n_+(z,t) - n_-(z,t) \right], \tag{5}$$

that has to be solved together with Eq. (1), by considering that $V(\pm d/2, t) = V_0 e^{i\omega t}$, where V_0 is small enough to assure the validity of the linear approximation and ω is the frequency

of the applied voltage. These equations govern the dynamics of the system and, after solving them, the impedance of the cell can be analytically established [4], in the form

$$Z = \frac{2}{i\omega\varepsilon S\beta^2}\left[\frac{\tanh(\beta \mathrm{d}/2)/(\lambda^2\beta) + \mathrm{Ed}/(2\mathrm{D})}{1 + (i\omega)^{\eta-1}\kappa(i\omega)(1 + i\omega\lambda^2/D)\tanh(\beta d/2)/(\lambda^2\beta)}\right], \tag{6}$$

where S is the surface of the electrodes and λ is the Debye's screening length. In Eq. (6), the other quantities are

$$\beta = \sqrt{\frac{F(i\omega)}{D} + \frac{1}{\lambda^2}}, \quad \text{with} \quad F(i\omega) = \int_0^\infty d\gamma\,\tau(\gamma)(i\omega)^\gamma, \tag{7}$$

and $E = F(i\omega) + \beta(i\omega)^\eta\kappa(i\omega)\tanh(\beta d/2)$. The transformed kernel is given by

$$\kappa(i\omega) = e^{-i\omega t}\int_0^\infty dt' k(t - t')e^{i\omega t'}. \tag{8}$$

The presence of this kernel $k(t - t')$ and of the fractional time derivative on the boundary condition give to the electrical impedance (6) a general profile. As a matter of fact, for $\tau(\gamma) = \delta(\gamma - 1)$, $\eta = 1$, with $k(t) = \kappa e^{-t/\tau}$, the case worked out in [1], in which adsorption-desorption phenomena are incorporated to the analysis by means of a kinetic balance equation at the surfaces, is recovered. On the other hand, for $\tau(\gamma) = \delta(\gamma - 1)$, with $k(t) = 0$, the usual form of the electrical impedance obtained in the situation of blocking electrodes is re-obtained.

4. Fitting Process

To analyse the experimental data, we have particularized the general expressions stated in the preceding Section to $\eta = 1$, $S = 10^{-4}$ m^2, and performed a choice for the two diffusion regimes as

$$F(i\omega) = a(i\omega) + b(i\omega)^\gamma, \tag{9}$$

where a (measured in s) and b (measured in s^γ) are the weights of the usual and the anomalous diffusion regimes, respectively. For the boundary conditions, we have used a transformed kernel given by

$$\kappa(i\omega) = \kappa\tau\left[\frac{1}{(i\omega\tau)^\vartheta} + \frac{\kappa_1}{\kappa}\frac{1}{(i\omega\tau)^{\vartheta_1}}\right], \tag{10}$$

in which ϑ and ϑ_1 are adjustable parameters. In (10), τ is a relaxation time (here measured in s), κ and κ_1 are phenomenological parameters (here measured in m/s) such that $\kappa\tau$ and $\kappa_1\tau$ are two characteristic lengths. In this framework, Eq. (10) involves the diffusion regimes occurring along two distinct regions near the surface, i.e., one layer of thickness $\kappa\tau$, characterized by an exponent ϑ, and another one of thickness $\kappa_1\tau$, characterized by an exponent ϑ_1. Thus, ϑ and ϑ_1 may be connected to the range of the interactions governing the dynamics of the mobile charges in these two layers.

From the initial numerical adjustments of the experimental data we have noticed that fixing the values of some parameters of the model the fitting process yielded good results. Taking this feature into account, the fit procedure was carried out in the following manner: the parameters λ, D, κ, κ_1, and τ have been used to adjust AU2, AU10, and ITO2

Table 2. Best fit parameter values for AU2, AU10, and ITO2 samples. The fixed values for this fit procedure were: $\varepsilon = 8.0\varepsilon_0$, $a = 1.0$, $b = 0$, $\vartheta = 0.25$, and $\vartheta_1 = 0.5$. All the parameters are expressed in SI units.

Parameter	AU2	AU10	ITO2
$\lambda(10^{-7})$	0.4560	1.0518	1.5276
$\kappa\tau(10^{-6})$	0.5940	1.2894	0.4908
$\kappa_1\tau(10^{-7})$	1.7428	5.8241	6.6626
$D(10^{-11})$	0.2049	0.5254	0.5868
$\kappa(10^{-6})$	0.8232	1.7200	0.3537
$\kappa_1(10^{-7})$	2.4153	7.7686	4.8019
τ	0.7216	0.7497	1.3875

experimental results; for ITO10 and ITO20 samples the parameters λ, D, κ, and τ are left free in the numerical routine.

In Tables 2 and 3 we summarize the parameter values that give the best fit for the experimental data worked here.

The following Figs. 3 and 4 show the experimental data with the fitting curves obtained by using Eqs. (6), (9), and (10), and the fitted parameters exhibited in Tables 2 and 3.

The fitting process shows that the behavior of the ITO sample with the thinner Polyimide layer (ITO2) is more alike to the AU2 and AU10 samples, as shown in Table 2. Indeed, when these results are compared with the ones shown in Table 3, it follows that the effective "surface lengths" of the ITO samples are about two orders of magnitude lower than the ones of the samples of Table 2. The parameter responsible for this substantial difference is τ, because κ remains of the order of 1 μm for all the analysed samples. In addition, to account for the behavior of AU samples, the kernel of Eq. (10) has to be assumed as a superposition of two terms. In this regard, it is noteworthy that the expected behavior of this term, when a first order kinetic equation (Langmuir approximation) is used as the balance equation at the surface [9], would be as $1/(i\omega\tau)$, i.e., $\vartheta = 1$ and $\kappa_1 = 0$ in Eq. (10). Since $b = 0$ in the fitting process, by means of Eq. (9) one concludes that it is not necessary to consider anomalous diffusive regimes in the bulk to obtain a best fit for the experimental data when gold electrodes or ITO electrodes with very thin Polyimide layer are used. However, it is mandatory to consider non-usual or "anomalous" response behavior at the interface to account for the trends of the experimental results.

Table 3. Best fit parameter values for ITO10 and ITO20 samples. The fixed values for this fit procedure were: $\varepsilon = 8.0\varepsilon_0$, $a = 1.0$, $b = 0$, $\vartheta = 0.2$, and $\kappa_1 = 0$. All the parameters are expressed in SI units.

Parameter	ITO10	ITO20
$\lambda(10^{-7})$	0.9706	1.0828
$\kappa\tau(10^{-9})$	5.7902	4.6488
$D(10^{-11})$	0.4854	1.5022
$\kappa(10^{-6})$	1.7882	0.6099
$\tau(10^{-3})$	3.2380	7.6223

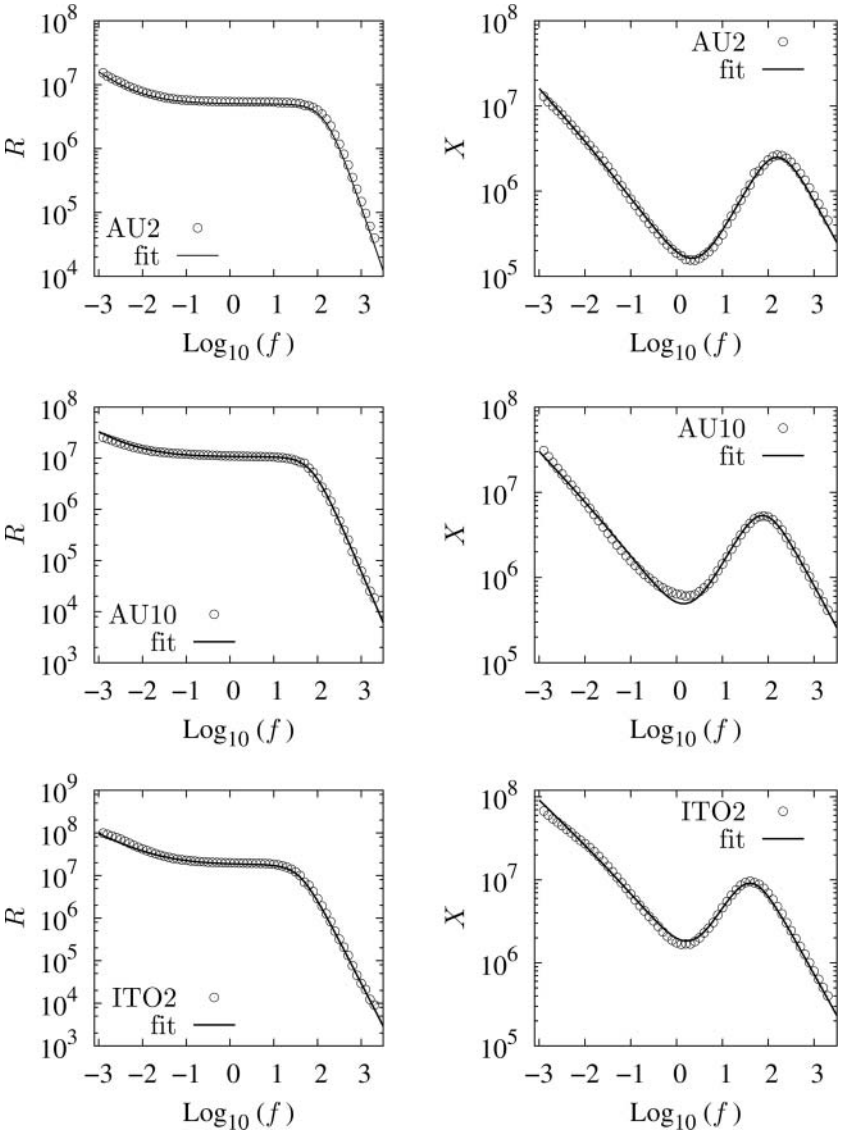

Figure 3. Experimental data and fitting curves for the real (R) and imaginary (X) parts of the impedance Z of the AU2, AU10, and ITO2 samples.

In the framework of the present model, we could interpret the results of Table 2 in a summarized way as follows. The bulk diffusion of ions can be described by the usual diffusion equation, while near to the electrodes we have a sophisticated diffusion process in which intervene two effective lengths, $\kappa\tau \approx 1$ μm and $\kappa_1\tau \approx 0.1$ μm. In samples having a thickness of the order of 30−35 μm as the one we are analysing here, these lengths are clearly much greater than the thickness of the Polyimide layer. One is then tempted to interpret these findings as an indication that the charges located near the interface of the highly conducting electrodes may undergo more than one anomalous diffusive regimes. The same conclusion holds true for the AU20 sample, as discussed in Ref. [8]. Thus, there

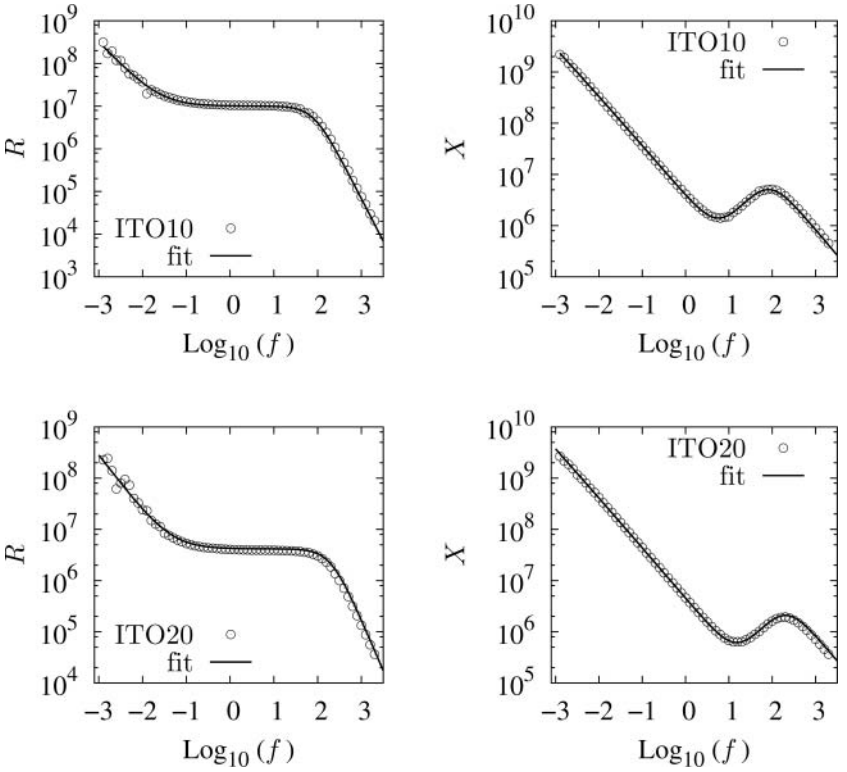

Figure 4. Experimental data and fitting curves for the real (R) and imaginary (X) parts of the impedance Z of the ITO10 and ITO20 samples.

are indications that the polyimide influences the behavior at low frequencies through the adsorption and desorption effects at the interface. The magnitude of effective resistance depends on the number of ions released by polyimide layers. Concerning the effective capacitance of the cell, the relaxation times decrease with the thickening of polyimide layer.

Looking now at the surface lengths shown in Table 3, one observes that $\kappa\tau \approx 1$ nm, i.e., the effective "surface length" is comparable with the thickness of the Polyimide layer, which is of the order of a few nano meters. In addition, it was not necessary to consider a second effective "surface length" for these samples, i.e., $\kappa_1\tau = 0$. Notwithstanding, the surface response behavior is also anomalous, and the transformed kernel is of the form $\kappa(i\omega) \approx (i\omega\tau)^{-1/5}$. In conclusion, it is possible to think that the charges near the electrodes of these ITO samples undergo a single, even if anomalous, diffusion regime.

5. Concluding Remarks

A simple and new conclusion emerges from the rapid analysis we have done here and can be stated as follows. While it is not necessary to account for anomalous diffusion regimes in the middle of the samples, i.e., far away from the surface, near to the interfaces these LC samples require a more involving theoretical treatment. To account for the rich behavior of the electrical impedance response of these systems it may or may not be necessary, but

will be surely useful, to consider anomalous response behavior at the interface. This can be accomplished by formulating the boundary conditions in such a way that they embody anomalous as well as conventional process. In this sense, by using the framework of the model presented here we have obtained a set of "surface lengths" that enabled us to perceive the existence of these anomalous process. We consider that this result can be useful to gain understanding of the phenomena that take place at the interface of these systems.

Acknowledgment

This work was partially supported by the National Institutes of Science and Technology (INCT-CNPq) of Complex Systems (E. K. L.), Complex Fluids (L. R. E.).

References

[1] Barbero, G., & Evangelista, L. R. (2006). *Adsorption Phenomena and Anchoring Energy in Nematic Liquid Crystals*, Taylor & Francis: London.
[2] Jakli, A., & Saupe, A. (2006). *One- and two-dimensional fluids*, CRC Press: Boca Raton.
[3] Yang, D-Ke., & Wu, S-Tson (2006). *Fundamentals of Liquid Crystal Devices*, Wiley-SID: Chichester.
[4] Santoro, P. A., de Paula, J. L., Lenzi, E. K., & Evangelista, L. R. (2011). *J. Chem. Phys.*, *135*, 114704.
[5] Podlubny, I. (1999). *Fractional Differential Equations*, Academic Press: San Diego.
[6] Zola, R. S., Lenzi, E. K., Evangelista, L. R., & Barbero, G. (2007). *Phys. Rev. E*, *75*, 042601.
[7] Zola, R. S., Freire, F. C. M., Lenzi, E. K., Evangelista, L. R., & Barbero, G. (2007). *Chem. Phys. Lett.*, *438*, 144.
[8] Ciuchi, F., Mazzulla, A., Scaramuzza, N., Lenzi, E. K., & Evangelista, L. R. (2012). *J. Phys. Chem. C.*, *116*, 8773.
[9] de Paula, J. L., Santoro, P. A., Zola, R. S., Lenz, E. K., Evangelista, L. R., Ciuchi, F., Mazzulla, A., & Scaramuzza, N. (2012). *Phys. Rev. E*, *86*, 051705.
[10] Lenzi, E. K., Evangelista, L. R., & Barbero, G. (2009). *J. Phys. Chem. B.*, *113*, 11371.
[11] Macdonald, J. R., Evangelista, L. R., Lenzi, E. K., & Barbero, G. (2011). *J. Phys. Chem. C.*, *115*, 7648.